

## Resonant x-ray emission spectroscopy of multiferroic TbMnO<sub>3</sub>

J. M. Chen,<sup>a)</sup> C. K. Chen, T. L. Chou, I. Jarrige, H. Ishii, K. T. Lu, Y. Q. Cai, and K. S. Liang  
National Synchrotron Radiation Research Center, Hsinchu 30076, Taiwan, Republic of China

J. M. Lee, S. W. Huang, and T. J. Yang  
Department of Electrophysics, National Chiao Tung University, Hsinchu 30076, Taiwan, Republic of China

C. C. Shen and R. S. Liu  
Department of Chemistry, National Taiwan University, Taipei 10617, Taiwan, Republic of China

J. Y. Lin  
Institute of Physics, National Chiao Tung University, Hsinchu 30076, Taiwan, Republic of China

H. T. Jeng  
Institute of Physics, Academia Sinica, Taipei 11529, Taiwan, Republic of China

C.-C. Kao  
Brookhaven National Laboratory, Upton, New York 11973

(Received 16 March 2007; accepted 30 June 2007; published online 1 August 2007)

The Mn 3*d* valence states in single-crystalline TbMnO<sub>3</sub> were probed using x-ray absorption spectroscopy and resonant x-ray emission spectroscopy (RXES). The polarized Mn *K*-edge x-ray absorption spectra show a strong polarization dependence, particularly for the white line region, indicating the strong anisotropic Mn–O bonding within the *ab* plane in TbMnO<sub>3</sub>. The RXES data obtained at the Mn *K* edge clearly reveal that unoccupied Mn 3*d* states exhibit a relatively delocalized character, stemming from hybridization of the Mn 3*d* states with the neighboring Mn 4*p* orbitals. The authors demonstrated that resonant x-ray emission spectroscopy is able to characterize the degree of localization of the unoccupied states or hole carriers in manganites. © 2007 American Institute of Physics. [DOI: 10.1063/1.2762288]

Multiferroic materials, in which two or more properties among (anti-)ferroelectricity, (anti-)ferromagnetism, and (anti-)ferroelasticity coexist, have recently sparked a surge of interest due to their potential applications in novel magneto-electric and magneto-optical devices using magnetoelectric (ME) effect.<sup>1</sup> The multiferroicity has been observed recently in manganites such as TbMnO<sub>3</sub>, DyMnO<sub>3</sub>, and TbMn<sub>2</sub>O<sub>5</sub>.<sup>2–5</sup> In this letter we focus on TbMnO<sub>3</sub>. TbMnO<sub>3</sub> exhibits the orthorhombically distorted perovskite structure at room temperature, and shows an incommensurate lattice modulation at the Néel temperature ( $T_N=42$  K) corresponding to a sinusoidal antiferromagnetic (AF) ordering. The transition to nearly-lock-in incommensurate antiferromagnetic phase ( $T_{\text{lock}}\sim 27$  K) is accompanied by ferroelectric ordering with a polarization  $P\parallel c$ . The ME phase diagram of TbMnO<sub>3</sub> varies substantially according to the crystallographic axis along which the magnetic field is applied.<sup>6</sup> The quest to understand the origin of multiferroicity has stimulated great interest in the magnetic, structural, and dielectric properties of the multiferroic materials.

As previously indicated by theoretical calculations in undoped manganites, a magnetically incommensurate phase of  $RMnO_3$  ( $R$ =rare earth) might reflect a competition between the Mn 3*d* antiferromagnetic superexchange interaction (including  $e_g^1$ -O- $e_g^1$  along the *ab* plane,  $e_g^0$ -O- $e_g^0$  along the *c* axis, and three-dimensional  $t_{2g}^3$ -O- $t_{2g}^3$ ) and the Mn 3*d* ferromagnetic superexchange interaction ( $e_g^1$ -O- $e_g^0$  along the *ab* plane).<sup>7–10</sup> The superexchange interactions between the Mn 3*d* states in  $RMnO_3$  are closely related to the hybridization of the Mn 3*d* orbitals with neighboring orbitals such as the O

2*p* states and the Mn 4*p* orbitals.<sup>11,12</sup> Based on band structure calculations, Elfimov *et al.* proposed the hybridization of extended Mn 4*p* states with neighboring Mn 3*d* orbitals to be a major factor in the anomalous x-ray scattering at the Mn *K* edge in manganites.<sup>11</sup> Moreover, on-site Mn 4*p*-3*d* hybridization in manganites was artificially introduced to account for an increased intensity in the Mn *K*-edge preedge region for Mn in a tetrahedral coordination site relative to an octahedral coordination site.<sup>13</sup> The Mn 4*p*-Mn 3*d* hybridization is expected to be correlated to the relatively delocalized character of the unoccupied Mn 3*d* states in  $RMnO_3$ , due to the large radial extent of the Mn 4*p* states. However, no clear-cut experimental evidence of the delocalization of the unoccupied Mn 3*d* states nor of the hybridization of the unoccupied Mn 3*d* states with the Mn 4*p* orbitals in manganites has been provided.<sup>13</sup>

Although numerous studies can be found on the structural, magnetic, and dielectric properties of TbMnO<sub>3</sub>,<sup>3,6,14,15</sup> the electronic structure and especially the degree of localization of the Mn 3*d* states in TbMnO<sub>3</sub> has not been investigated in detail. In this study, we investigated the hybridization of Mn 3*d* states in TbMnO<sub>3</sub> using x-ray absorption spectroscopy and resonant x-ray emission spectroscopy. We observed a strong polarization dependence of the Mn *K*-edge x-ray absorption spectra, particularly for the white line region. The 1*s*3*p* resonant x-ray emission spectroscopy (RXES) spectra obtained at the Mn *K* preedge for TbMnO<sub>3</sub> clearly reveal that the unoccupied Mn 3*d* states exhibit a relatively delocalized character, indicated to originate from the hybridization of the unoccupied Mn 3*d* states with the Mn 4*p* orbitals.

Untwined high-quality TbMnO<sub>3</sub> single crystals were grown by the high-temperature solution growth method with

<sup>a)</sup> Author to whom correspondence should be addressed; electronic mail: jmchen@nsrrc.org.tw

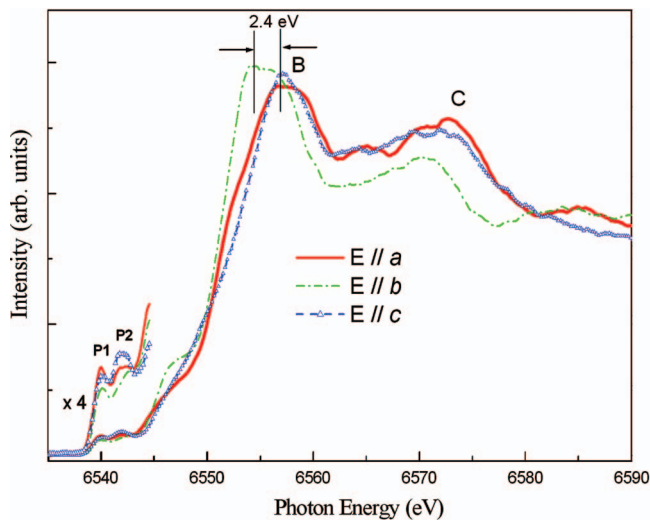


FIG. 1. (Color) Polarization-dependent Mn  $K$ -edge x-ray absorption spectra of single-crystalline  $\text{TbMnO}_3$  for polarizations  $E \parallel a$ ,  $E \parallel b$ , and  $E \parallel c$  at  $\sim 10$  K measured by partial fluorescence yield at the  $K\beta_{13}$  line. The pre-edge peaks P1 and P2 are shown enlarged.

the use of  $\text{PbF}_2$  flux in a Pt crucible. The crystal surfaces of the crystallographic directions of (001), (010), and (100) were prepared using an x-ray diffractometer. The Mn  $K$ -edge x-ray absorption spectra and Mn  $1s3p$ -RXES spectra were performed at the Taiwan Beamline BL12XU at SPring-8 in Japan. The emitted x-ray fluorescence was analyzed using a Si (440) spherically bent analyzer of 1 m radius. The overall resolution was estimated to be  $\sim 0.9$  eV from the full width at half maximum of the elastic peak measured at the Mn  $K\beta_{13}$  emission energy,  $\sim 6492$  eV.

Figure 1 shows polarized Mn  $K$ -edge high-resolution x-ray absorption spectra of single-crystalline  $\text{TbMnO}_3$  measured at  $\sim 10$  K for the polarizations  $E \parallel a$ ,  $E \parallel b$ , and  $E \parallel c$ . The absorption spectra were obtained in the partial-fluorescence-yield mode, with the spectrometer energy fixed at the maxi-

imum of the Mn  $K\beta_{13}$  line. The Mn  $K$ -edge x-ray absorption spectra consist of two well resolved peaks in the pre-edge region (P1 and P2 in Fig. 1) and intense white line on the site of greater photon energy (B in Fig. 1). These pre-edge features are generally ascribed to quadrupole  $1s$ - $3d$  and/or modifications of the dipole transition probability due to the hybridization between  $3d$  and  $4p$  states. There have been a large number of papers in addressing these issues for many transition metals, not all of which are in agreement.<sup>16–18</sup> The interpretation of the pre-edge features remains controversial. The present work reveals the nature of the pre-edge peaks P1 and P2, as discussed in the following paragraphs. The main line (peak B in Fig. 1) is related to the  $1s$  to  $4p$  transitions. Feature C gains intensity from the multiple scattering contribution of  $\text{MnO}_6$  surrounded by eight Tb. As shown in Fig. 1, the Mn  $K$ -edge x-ray absorption spectra exhibit a significant anisotropy along the three crystallographic directions, particularly for the main line region (peak B). As noted, a substantial difference in the spectral shape and energy of the main line is observed among the polarizations, especially for  $E \parallel b$  compared with  $E \parallel a$  and  $E \parallel c$ . An energy shift  $\sim 2.4$  eV is measured for the maximum of the main line of the spectrum obtained along  $E \parallel b$  relative to  $E \parallel a$  and  $E \parallel c$ . This implies the strong anisotropic Mn–O bonding within the  $ab$  plane in  $\text{TbMnO}_3$  and relatively weak covalency along the  $b$  axis, as supported by polarization-dependent O  $K$ -edge x-ray absorption spectra of single-crystalline  $\text{TbMnO}_3$ .<sup>19</sup> The origin of this energy difference is reminiscent of the Jahn-Teller distortion of the  $\text{MnO}_6$  octahedra and the Coulomb repulsion between the occupied  $3d$  orbital and the  $4p$  orbitals.<sup>11,20</sup> Due to the strong anisotropic Mn–O bonding within the  $ab$  plane in  $\text{TbMnO}_3$ , the superexchange interactions along the  $a$  and  $b$  directions become inequivalent. Through the large tilting in  $\text{TbMnO}_3$ , the relatively weak overlap between the Mn  $3d$   $e_g$  and the O  $2p$  orbitals along the  $b$  axis, as shown in Fig. 1, is too small to provide a strongly ferromagnetic (FM) superex-

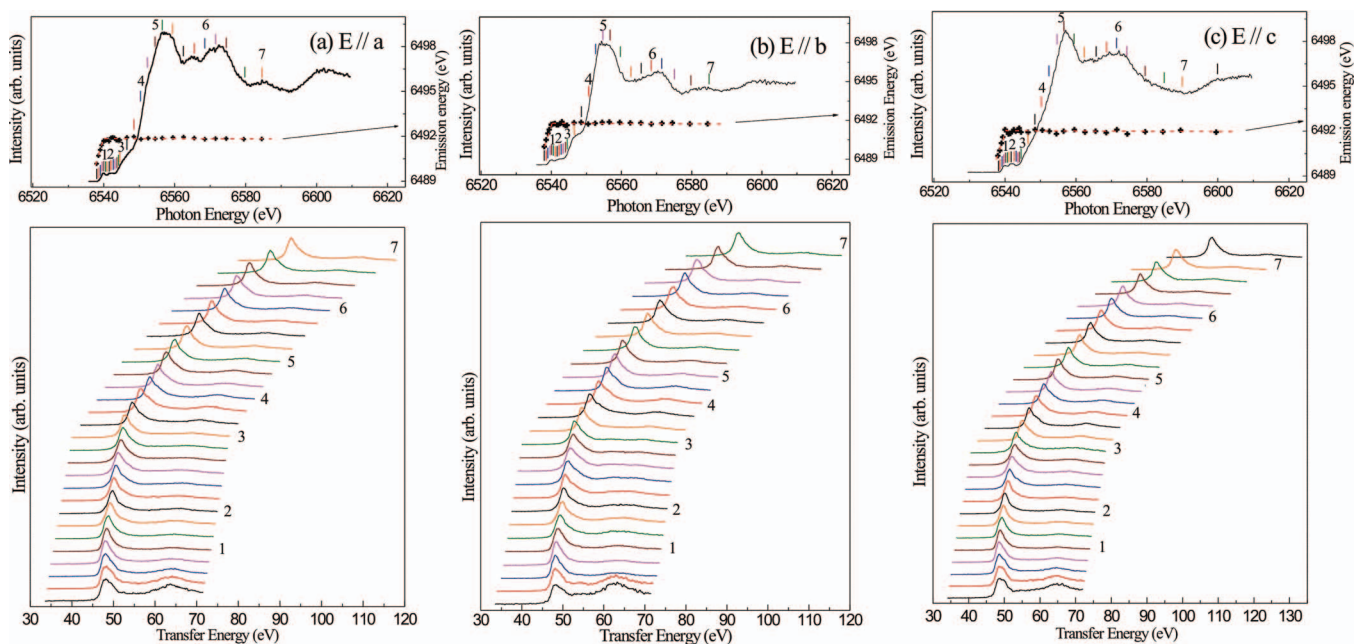


FIG. 2. (Color)  $1s3p$  resonant x-ray emission spectra of single-crystalline  $\text{TbMnO}_3$  measured at  $\sim 10$  K as a function of transfer energy for polarizations (a)  $E \parallel a$ , (b)  $E \parallel b$ , and (c)  $E \parallel c$ . The resonant x-ray emission spectra are plotted from bottom to top in increasing incident photon energies. Ticks in the Mn  $K$ -edge absorption spectrum shown in the top panels indicate the excitation energies at which the resonant x-ray emission spectra were recorded. The number indicated in the emission spectra corresponds to the excitation energy marked in the Mn  $K$ -edge x-ray absorption spectra. The emission energy at the  $K\beta_{13}$  line in the emission spectra as a function of the incident energy along three crystallographic directions is plotted in the top panels (crosses, right scale).

change between Mn cations. Thus, the competition between the antiferromagnetic  $e_g^1\text{-O-}e_g^1$  (and  $t_{2g}^3\text{-O-}t_{2g}^3$ ) interaction and the ferromagnetic  $e_g^1\text{-O-}e_g^0$  interaction calls for a subtle balance of magnetic superexchange interactions and leads to complex incommensurate modulated magnetic structures along the  $b$  axis below  $T_{\text{lock}}$ .<sup>6,7</sup>

The  $1s3p$ -RXES spectra obtained for single-crystalline  $\text{TbMnO}_3$  at  $\sim 10$  K are shown in Fig. 2 for the polarizations  $E\parallel a$ ,  $E\parallel b$ , and  $E\parallel c$ . The RXES spectra are plotted as a function of transfer energy, and ordered from bottom to top in increasing incident photon energies. Ticks in the Mn  $K$ -edge x-ray absorption spectrum indicate the excitation energies at which the RXES spectra were recorded. We analyzed the RXES data in terms of quadrupolar transitions to  $1s^{-1}3d^{m+1}$  intermediate states or dipolar-assisted transitions to  $1s^{-1}3d^n4p^1$  intermediate states, which are primarily assigned to the preedge and white line spectral regions. The final states are reached by decay of a  $3p$  electron, leading to the  $3p^{-1}3d^{m+1}$  or  $3p^{-1}3d^n4p^1$  configuration. For simplicity we here neglect multielectronic effects and configuration interaction.<sup>21</sup>

As clearly seen in Fig. 2, the features related to transitions to the localized intermediate  $1s^{-1}3d^{m+1}$  states appear at a constant transfer energy, characteristic of the so-called Raman regime.<sup>13</sup> Fluorescencelike features, corresponding to the delocalized  $3p^{-1}3d^n4p^1$  final states, appear at a linearly dispersed transfer energy with the incident energy. The whole series of RXES spectra was fitted with a sum of Voigt functions. The emission energy of the fluorescence line provided by the fitting of the RXES spectra is plotted as a function of the incident energy in the top panels of Fig. 2 (crosses, right scale). The inclined line indicates the Raman region, whereas the horizontal one corresponds to the fluorescence regime. Especially noteworthy from Fig. 2 is that the Raman regime is only limited to below the preedge. The fluorescence regime starts from the first prepeak of  $1s \rightarrow 3d$  transitions, indicating the delocalization of intermediate  $1s^{-1}3d^{m+1}$  states and thus a relatively delocalized character of unoccupied Mn  $3d$  states.

A reasonable explanation for the delocalization of intermediate  $1s^{-1}3d^{m+1}$  states via  $1s \rightarrow 3d$  transitions originates from the hybridization between Mn  $3d$  and Mn  $4p$  orbitals, of which the latter belongs to the photon-absorbing Mn atom or to a neighboring Mn atom. We found that the relatively delocalized character of the unoccupied Mn  $3d$  states was observed even in nearly octahedral structure of  $\text{Tb}_{0.15}\text{Ca}_{0.85}\text{MnO}_3$ , for which the contribution of on-site Mn  $3d$ - $4p$  hybridization is negligible.<sup>19</sup> Accordingly, it is expected that hybridization between Mn  $3d$  orbitals and neighboring Mn  $4p$  states in  $\text{TbMnO}_3$  makes a major contribution to preedge structures in Mn  $K$ -edge x-ray absorption spectrum. Based on the calculations of band structure in  $\text{LaMnO}_3$ , Elfimov *et al.* proposed that the central Mn  $4p$  orbitals hybridize either directly or via the intervening O  $2p$  orbitals with the neighboring Mn  $3d$  orbitals.<sup>11</sup> The present RXES fully agrees with this hypothesis.

To ensure a proper assignment of the preedge features P1 and P2 in Fig. 1, we performed local density approximation plus on-site Coulomb interaction  $U$  (LDA+ $U$ ) band structure calculations of  $\text{TbMnO}_3$ .<sup>19</sup> P1 in Fig. 1 is ascribed to the transition into unoccupied majority-spin  $e_g^{\uparrow}$  states hybridized with the Mn  $4p$  states. The direct coupling strength of

the off-axis  $t_{2g}$  states with the  $4p$  orbitals is proposed to be negligible.<sup>11,20</sup> However, based on polarized O  $K$ -edge x-ray absorption spectra of  $\text{TbMnO}_3$  single crystals, strong hybridization of the Mn  $t_{2g}\downarrow$  and the O  $2p$  orbitals was observed particularly for  $E\parallel c$ .<sup>19</sup> As shown in Fig. 1, the intensity of the P2 peak is stronger for  $E\parallel c$  relative to  $E\parallel a$  and  $E\parallel b$ . It appears that the  $t_{2g}\downarrow$  orbitals, hybridized indirectly with the neighboring Mn  $4p$  states through the O  $2p$  states, contribute to the P2 peak. We therefore suggest that P2 in Fig. 1 is assigned as a superposition of the transition into empty minority-spin  $t_{2g}\downarrow$  and  $e_g\downarrow$  states hybridized with the  $4p$  states.

In conclusion, we investigated the Mn  $3d$  valence states in single-crystal  $\text{TbMnO}_3$  by combining x-ray absorption spectroscopy and RXES. The polarized Mn  $K$ -edge x-ray absorption spectra show a strong polarization dependence, particularly for the white line region, originating from the strong anisotropic Mn–O bonding within the  $ab$  plane in  $\text{TbMnO}_3$ . The highly anisotropic Mn–O bonding is closely related to the complex incommensurate modulated magnetic structures in  $\text{TbMnO}_3$ . The RXES spectra obtained at the Mn  $K$  edge clearly reveal that the unoccupied Mn  $3d$  states exhibit a relatively delocalized character as a consequence of the hybridization of the unoccupied Mn  $3d$  states with the neighboring Mn  $4p$  orbitals. We clearly demonstrated that with resonant x-ray emission spectroscopy one can characterize successfully the degree of localization of the unoccupied states or hole carriers in manganites.

This research is supported by the NSRRC and the National Science Council of Taiwan under Grant No. NSC 95-2113-M-213-001.

<sup>1</sup>M. Fiebig, J. Phys. D **38**, R123 (2005).

<sup>2</sup>T. Kimura, T. Goto, H. Shintani, K. Ishizaka, T. Arima, and Y. Tokura, Nature (London) **426**, 55 (2003).

<sup>3</sup>T. Goto, T. Kimura, G. Lawes, A. P. Ramirez, and Y. Tokura, Phys. Rev. Lett. **92**, 257201 (2004).

<sup>4</sup>N. Hur, S. Park, P. A. Sharma, J. S. Ahn, S. Guha, and S.-W. Cheong, Nature (London) **429**, 392 (2004).

<sup>5</sup>L. C. Chapon, G. R. Blake, M. J. Gutmann, S. Park, N. Hur, P. G. Radaelli, and S.-W. Cheong, Phys. Rev. Lett. **93**, 177402 (2004).

<sup>6</sup>T. Kimura, G. Lawes, T. Goto, Y. Tokura, and A. P. Ramirez, Phys. Rev. B **71**, 224425 (2005).

<sup>7</sup>J.-S. Zhou and J. B. Goodenough, Phys. Rev. Lett. **96**, 247202 (2006).

<sup>8</sup>J. Salafranca and L. Brey, Phys. Rev. B **73**, 024422 (2006).

<sup>9</sup>T. Kimura, S. Ishihara, H. Shintani, T. Arima, K. T. Takahashi, K. Ishizaka, and Y. Tokura, Phys. Rev. B **68**, 060403 (2003).

<sup>10</sup>I. A. Sergienko and E. Dagotto, Phys. Rev. B **73**, 094434 (2006).

<sup>11</sup>I. S. Elfimov, V. I. Anisimov, and G. A. Sawatzky, Phys. Rev. Lett. **82**, 4264 (1999).

<sup>12</sup>J. B. Goodenough, J. Appl. Phys. **81**, 5330 (1997).

<sup>13</sup>J.-P. Rueff, L. Journel, P.-E. Petit, and F. Farges, Phys. Rev. B **69**, 235107 (2004).

<sup>14</sup>R. Kajimoto, H. Yoshizawa, H. Shintani, T. Kimura, and Y. Tokura, Phys. Rev. B **70**, 012401 (2004).

<sup>15</sup>T. Arima, T. Goto, Y. Yamasaki, S. Miyasaka, K. Ishii, M. Tsubota, T. Inami, Y. Murakami, and Y. Tokura, Phys. Rev. B **72**, 100102 (2005).

<sup>16</sup>A. Yu. Ignatov, N. Ali, and S. Khalid, Phys. Rev. B **64**, 014413 (2001).

<sup>17</sup>H. Hayashi, A. Sato, T. Azumi, Y. Udagawa, T. Inami, K. Ishii, and K. B. Garg, Phys. Rev. B **73**, 134405 (2006).

<sup>18</sup>Q. Qian, T. A. Tyson, S. Savrasov, C.-C. Kao, and M. Croft, Phys. Rev. B **68**, 014429 (2003).

<sup>19</sup>J. M. Chen, J. M. Lee, S. W. Huang, H. T. Jeng, C. K. Chen, K. T. Lu, T. J. Yang, C. C. Shen, R. S. Liu, and K. S. Liang (unpublished).

<sup>20</sup>L. Hozoi, A. H. de Vries, and R. Broer, Phys. Rev. B **64**, 165104 (2001).

<sup>21</sup>T. E. Westre, P. Kennepohl, J. G. DeWitt, B. Hedman, K. O. Hodgson, and E. I. Solomon, J. Am. Chem. Soc. **119**, 6297 (1997).